

# Final result at the Muon $g-2$ experiment at Fermilab

Elia Bottalico,<sup>1\*</sup>

<sup>1</sup>University of Liverpool, L69 7ZE, Liverpool, UK

## Abstract

The Muon  $g - 2$  experiment at Fermilab's goal was to determine the muon's magnetic moment anomaly with an unprecedented precision of 0.14 parts per million (ppm). The anomaly is extracted from the ratio of the muon's anomalous spin precession frequency in a magnetic storage ring to the magnetic field experienced by the ensemble of muons. In this talk, I will present the analysis of data collected from 2020 to 2023, which has achieved a precision of 139 parts per billion (ppb) and, when combined with previous results, leads to a new world average of 124 ppb [1]. I will show the result and discuss the experimental technique, the analysis details and the control of systematic effects that were decisive in achieving the final precision. This represents the most precise determination of the muon magnetic anomaly to date and provides a critical benchmark for testing the Standard Model at the highest precision.

*Keywords:*  $g-2$ , Lepton, high precision, standard model

*DOI:* 10.31526/PHEP.2025.26

## 1. INTRODUCTION

The magnetic moment of a lepton ( $l$ ) with spin  $s$ , charge  $q$ , mass  $m$  and gyromagnetic ratio  $g$  is defined as:

$$\vec{\mu}_l = g_l \left( \frac{q}{2m_l} \right) \vec{s}. \quad (1)$$

Dirac predicted  $g_l = 2$  for the electron (and, consequently, any spin  $\frac{1}{2}$  elementary particle) [2]. Schwinger proposed an additional contribution to the electron magnetic moment from a radiative correction, predicting the magnetic anomaly  $a_l = \frac{g_l - 2}{2} = \frac{\alpha}{2\pi} \simeq 0.00116$ , where  $\alpha$  is the fine structure constant, in agreement with experiment [3]. Subsequently, theoretical calculations within the Standard Model (SM) demonstrated how each sector contributes, through vacuum polarization, to the theoretical prediction of the muon magnetic anomaly,  $a_\mu$  [4].

In parallel, experimental precision measurements of the muon magnetic moment,  $g_\mu$ , have advanced over several decades, beginning with the pioneering experiments at Columbia University's Nevis Laboratory [5, 6] and the University of Liverpool [7]. Direct determinations of the muon anomaly,  $a_\mu$ , were subsequently performed at CERN in the CERN-I [8], CERN-II [9], and CERN-III [10] experiments, and were later refined by the E821 experiment at Brookhaven National Laboratory (BNL) [11]. The E821 results revealed a statistically significant deviation from the SM prediction at the time, motivating the development of a new, higher-precision experiment at Fermilab.

In the Muon  $g - 2$  Experiment at Fermilab, polarized muons, with a momentum of 3.1 GeV/ $c$ , are injected into a superconducting storage ring of 14 meters in diameter. While muons are collected in the storage ring and orbit with a frequency defined by the cyclotron frequency:

$$\vec{\omega}_C = \frac{e\vec{B}}{m\gamma}, \quad (2)$$

The torque on the magnetic moment, together with the Thomas precession, rotates the muon spin at the frequency [12]:

$$\vec{\omega}_S = g \frac{e}{2m} \vec{B} + (1 - \gamma) \frac{e\vec{B}}{\gamma m}. \quad (3)$$

By computing the difference between  $\vec{\omega}_C$  and  $\vec{\omega}_S$  in the laboratory frame, we obtain the rotation frequency of the muon spin relative to its momentum, known as the *anomalous precession frequency*  $\vec{\omega}_a$ . This frequency, together with the measurement of the storage-ring magnetic field, constitutes the most important observable of the  $g - 2$  experiment. The most general expression for  $\vec{\omega}_a$  is:

$$\vec{\omega}_a \approx \vec{\omega}_S - \vec{\omega}_C = \frac{e}{m} \left[ a_\mu \vec{B} - \left( a_\mu - \frac{1}{\gamma^2 - 1} \right) (\vec{\beta} \times \vec{E}) - a_\mu \left( \frac{\gamma}{\gamma + 1} \right) (\vec{\beta} \cdot \vec{B}) \vec{\beta} \right]. \quad (4)$$

We can simplify this expression and cancel the effect of the electric field by producing muons at the "magic momentum" of  $p_\mu = 3.094$  GeV/ $c$  which corresponds to  $\gamma = \sqrt{1 + \frac{1}{a_\mu}} \approx 29.3$ . With this choice  $a_\mu$  can be written as:

$$a_\mu = \frac{m \omega_a}{e B} \quad (5)$$

From Eq.5  $a_\mu$  is obtained as the ratio of the measured anomalous frequency and the magnetic field. At Fermilab experiment, this ratio is determined as  $R'_\mu = \omega_a / \tilde{\omega}'_p(T_r)$  where  $\tilde{\omega}'_p$  is the nuclear magnetic resonance (NMR) precession frequency of shielded protons in a spherical water sample (corrected to a reference temperature  $T_r$ ), where the tilde indicates it's averaged over the muon distribution, which expresses the magnetic field strength.

Both the measured frequencies  $\omega_a^m$  and  $\omega'_p(T_r) \times M$ , where  $\times M$  indicates that the measured magnetic field is weighted by the muon distribution, must be corrected for several effects via:

$$R'_\mu = \frac{\omega_a^m (1 + C_e + C_p + C_{pa} + C_{dd} + C_{ml})}{(\omega'_p(T_r) \times M) (1 + B_q + B_k)}. \quad (6)$$

$B_q$  corrects for vibrations of the Electrostatic Quadrupole (ESQ) system plates and  $B_k$  accounts for eddy currents generated by the fast injection kickers [13]. The combined effect of these corrections for Run-456 dataset is  $(-58 \pm 30)$  ppb. The corrections

\*Corresponding author: Elia.Bottalico@liverpool.ac.uk

$C_i$  affecting the anomalous precession frequency are divided into two groups. The first group accounts for residual contributions to the muon spin precession rate from the electric field  $C_e$  and from vertical betatron motion  $C_p$ . The second group arises from time-dependent changes in the mean phase of the observed muon ensemble, caused by (i) detector acceptance  $C_{pa}$ , (ii) phase-momentum correlations coupled to momentum-dependent muon lifetimes  $C_{dd}$ , and (iii) momentum-dependent muon storage losses  $C_{ml}$ . Collectively, these corrections shift the measured value of the anomalous precession frequency for Run-456 dataset by 515 ppb, with a total systematic uncertainty of 42 ppb [1]. Finally, once the unbiased  $R'_\mu$  is extracted the muon magnetic anomaly is obtained as:

$$a_\mu = R'_\mu \frac{\mu'_p(T_r)}{\mu_B} \frac{m_\mu}{m_e}, \quad (7)$$

where  $\mu'_p(T_r)/\mu_B$  is the ratio of the shielded proton magnetic moment to the Bohr magneton at  $T_r=25^\circ\text{C}$  and  $m_\mu/m_e$  is the muon-to-electron mass ratio<sup>†</sup>.

## 2. $\omega_A$ MEASUREMENT

In the Muon  $g - 2$  experiment at Fermilab, polarized muons are injected into a storage ring. Due to parity violation in weak muon decay, the resulting high energy positrons are emitted preferentially along the muon spin direction. These positrons are detected by 24 electromagnetic calorimeters, which measure their energies and arrival times. Each calorimeter consists of 54 lead-fluoride ( $\text{PbF}_2$ ) crystals read out by silicon photomultipliers (SiPMs). A state-of-the-art laser-based system is used to synchronize the detectors in time and correct for gain fluctuations [16]. Due to the large flux of particles hitting the calorimeters shortly after injection, the SiPMs experience significant gain fluctuations that, if not corrected, would introduce a systematic error in the measurement of the energy deposited in the calorimeters and consequently in  $\omega_a$ . In the E821 experiment, this effect led to the largest systematic uncertainty in the anomalous precession frequency fit, about 120 ppb. Thanks to the new system, the corresponding systematic uncertainty is now on the order of 10 ppb. In addition, two straw-tracker systems, consisting of 32 stereo modules made of drift tubes filled with a 50:50 Argon–Ethane gas mixture, are used to measure the beam profile in a non-destructive way, helping to evaluate related systematics. They are located at approximately  $180^\circ$  and  $270^\circ$  with respect to the beam injection point.

The  $\omega_a$  frequency is determined by reconstructing the time distribution of high-energy positrons. The simplest description of the positron time dependence is:

$$N(t) = N_0 \cdot e^{-t/\tau} \cdot (1 + A \cos(\omega_a \cdot t + \varphi_a)). \quad (8)$$

Due to the motion of the beam about the central orbit, a multiparameter fit function is needed to account for vertical ( $f_y$ ,  $f_{VW}$ ) and radial ( $f_{CBO}$ ) beam oscillations and muon losses that affect the determination of  $a_\mu$ . Such frequencies can be seen by the Fast Fourier Transform (FFT) of the fit residuals as shown in Fig. 1.

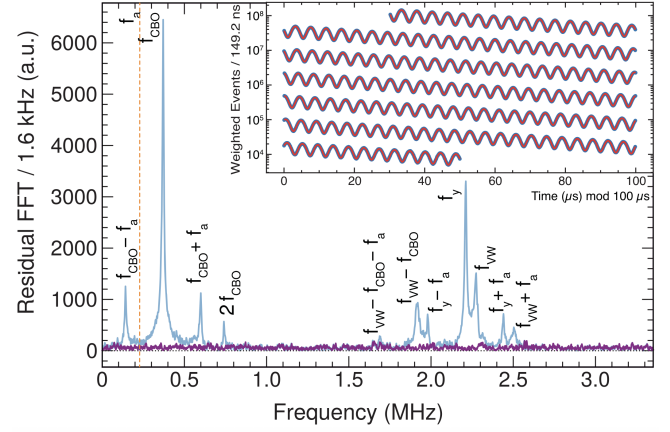


**FIGURE 1:** Fourier transform of the residuals from a fit using Eq. 8 (blue curve) and using a multiparameter function (purple line). The rf-driven CBO damping has decreased the power at  $f_{CBO}$  compared to earlier data. The dashed line (orange) indicates the anomalous precession frequency  $f_a$ . Inset: the asymmetry-weighted  $e^+$  time spectrum for the summed data (blue) and fit functions (red). [1]

The motion of the muons inside the storage ring is accurately modeled by a multi-parameter fit function, but Fig. 1 clearly shows that the radial CBO frequency has the strongest influence on the positron spectrum. In the  $g - 2$  experiment, strong vertical focusing is provided by the ESQ, which significantly suppresses vertical oscillations. Radially, only weak betatron focusing confines the muon beam, resulting in a large horizontal oscillation. In an ideal detector with uniform acceptance over the decay region, beam oscillations would not produce any modulation in the positron time spectrum. In a real detector, however, the decay-vertex-dependent acceptance introduces a time-dependent modulation in the positron time spectrum.

This led to one of the largest systematic uncertainties in the  $\omega_a$  measurement during Run-23 [15]. As one of the major improvements, during Run-4 data taking, an RF damping system was developed and tested to strongly reduce the horizontal oscillations [17]. Figure 2 illustrates the operation of the RF system. During Run-56, the transverse RF electric field, applied via the ESQ system, was used during data acquisition. This reduced the CBO amplitude by about an order of magnitude, lowering the overall bias on  $\omega_a$  (when not fitting for this oscillation) from approximately 800 ppb to about 100 ppb. Although this change significantly reduced the size of the effect, the associated uncertainty on the correction remained roughly the same. As a result, the relative uncertainty on the CBO contribution increased, but the overall systematic bias to  $a_\mu$  decreased, reflecting a smaller bias to correct in the measured value.

## 3. $\omega_P$ MEASUREMENT

The magnetic field is measured by a suite of pulsed-proton NMR probes. Every  $\sim 3$  days the data taking is stopped and a mobile set of 17-probe NMR probes, carried on a device called the trolley, measures the field at about 9000 locations in azimuth to provide a set of 2D field maps, while 378 pulsed NMR probes located outside the beam region continuously monitor

<sup>†</sup> $\mu'_p(T_r)/\mu_B = 1.5209931551(62) \times 10^{-3}$ ;  $m_\mu/m_e = 206.7682827(46)$ , both from [14]

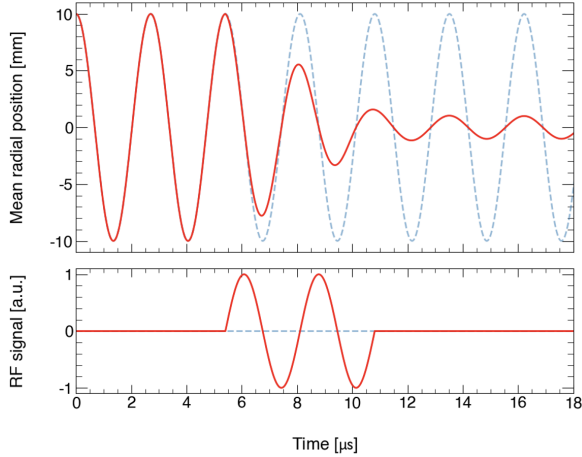


**FIGURE 2:** Illustration of the RF system signal (bottom) and the mean radial beam position as a function of time (top), before and after the application of the RF signal.

the field. The trolley is calibrated against shielded protons in a spherical water sample at a reference temperature  $T_r$ . The calibration procedure consists of two steps. First, the trolley probes are calibrated against a cylindrical, water-based calibration probe by comparing magnetic field differences under identical conditions inside the muon storage volume. Second, the calibration probe measurements are converted to absolute field values by applying corrections for the probe's magnetic environment. The combination of field maps from the trolley and continuous fixed probe measurements allows reconstruction of the magnetic field inside the storage volume as  $\omega'_p(x, y, \varphi, t)$ . To determine the magnetic field weighted by the muon distribution in time and space, the distribution measured by the trackers  $M(x, y)$  are used. The interpolated field maps are averaged over periods of roughly 10s and weighted by the number of detected positrons during the same period. We determine the muon-weighted average magnetic field by summing the field moments multiplied by the beam-weighted projections for every three-hour interval. In Fig. 3, the superposition of the azimuthally averaged field contours over the muon distribution is shown.

#### 4. FINAL RESULT

Given the extremely high precision of this experiment, a blinding procedure is essential to avoid bias. For this reason, a series of blinding mechanisms implemented at both the software and hardware levels are applied to ensure the most unbiased result possible. Before unveiling the final result, the collaboration meets and votes on the decision to unblind. Once unanimous consensus is reached, the final value is revealed. Fig. 4 shows the final result. The Run-456 result shows excellent agreement with the previous measurement, achieving a total precision of 139 ppb, obtained as the quadratic sum of a statistical uncertainty of 114 ppb and a systematic uncertainty of 76 ppb. Including all Muon  $g - 2$  data collected at Fermilab, the combined uncertainty is 127 ppb, with a statistical component of 98 ppb and a systematic component of 78 ppb. Table 1 shows the summary of the Fermilab measurements uncertainties.

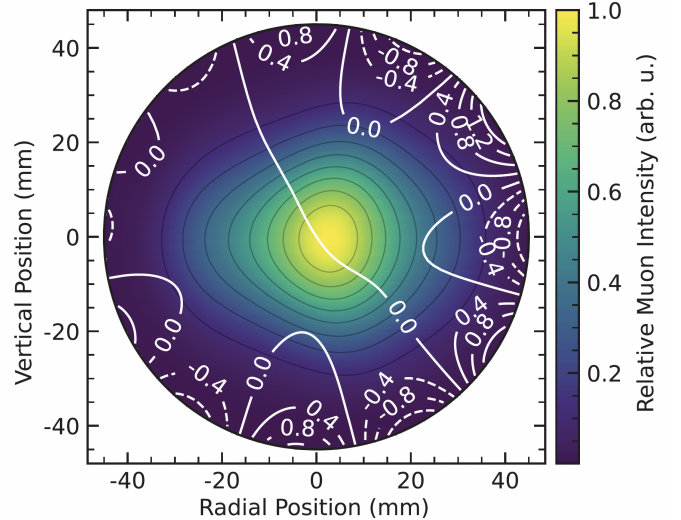


**FIGURE 3:** Azimuthally averaged magnetic field contours  $\omega'_p(x, y)$  overlaid on the time and azimuthally averaged muon distribution  $M(x, y)$  [1].

$\frac{\omega'_\mu}{\omega'_p}$	Stat. Unc. [ppb]	Syst. Unc. [ppb]	Total Unc.
Run-1	434	159	462
Run-23	201	78	216
Run-456	114	76	137
Run-1-6	98	78	125

**TABLE 1:** Uncertainties of the  $\frac{\omega'_\mu}{\omega'_p}$  ratio for all the datasets of Muon  $g - 2$  experiment at Fermilab. [1]

These results surpass the original design goal of 100 ppb for each statistical and systematic uncertainties. The Run-456 result is 1.8 times more precise than the Run-23 result [15], while the combined Run-1/6 average is 4.3 times more precise than the previous measurement at BNL [11].

The new muon anomaly experimental value resulting from the world average is:

$$a_\mu = 0.001165920715(145), \quad (9)$$

corresponding to a total precision of 124 ppb, which is 4.4 times more precise than the previous world average. This represents the most precise determination of the muon magnetic anomaly to date and provides a powerful benchmark for potential extensions of the Standard Model (SM).

From the theoretical side, the Muon  $g - 2$  Theory Initiative has released an updated SM prediction for  $a_\mu$  in their 2025 White Paper (WP2025) [4]. This new evaluation agrees with the current experimental average and represents a significant revision compared to the 2020 White Paper (WP2020) [18]. The shift arises primarily from the exclusive adoption of recently published leading-order hadronic vacuum polarization (HVP) estimates obtained from lattice-QCD calculations. In contrast, the WP2020 result relied on experimental measurements of  $e^+e^- \rightarrow$  hadrons cross sections from several experiments, evaluated via a dispersion relation, which yielded a prediction in tension with the measured value. More recent cross-section measurements [19] have increased the inconsistencies among the experimental datasets, leading the Theory Initiative to exclude a dispersion-based prediction from WP2025. Ongoing ef-

forts continue to refine the leading-order HVP contribution using both lattice-QCD and dispersion-integral approaches. Fig. 4 summarizes the current status of the theoretical determinations of the muon anomaly,  $a_\mu$ .

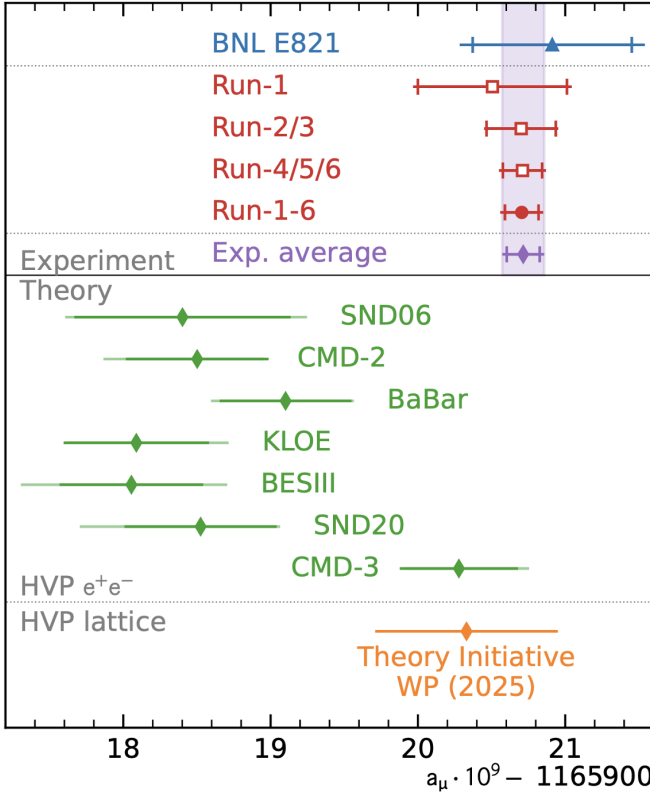


**FIGURE 4:** *Top:* Experimental values of  $a_\mu$  from BNL E821 [11] (blue triangle), and our results from Run-1 to Run-456 (red squares) [1], those three results combined (red circle), and the new experimental world average (purple diamond). The inner tick marks indicate the statistical contribution to the total uncertainties. *Bottom:* Theory values, dispersion-based prediction from experimental measurements of  $e^+e^- \rightarrow$  hadrons cross sections (green), new WP2025 result (orange) [4].

## 5. BSM SEARCH AT MUON $G - 2$ AT FERMILAB

The Muon  $g - 2$  experiment at Fermilab is designed to directly measure the muon anomalous magnetic moment. However, it also provides sensitivity to certain Beyond Standard Model (BSM) effects that can couple to the primary observable of the experiment, the anomalous precession frequency  $\omega_a$ . One observable that is directly related to  $\omega_a$  is the electric dipole moment (EDM). Leptonic EDMs violate parity (P) and time-reversal (T) symmetries and, under the assumption of CPT conservation, they represent an additional source of CP violation. To date, no EDM has been observed for any fundamental particle.

The EDM  $\vec{d}$  of a spin-1/2 particle can be written as:

$$\vec{d} = \eta \frac{q}{2mc} \vec{s} \quad (10)$$

where  $q$  is the charge,  $m$  the mass,  $c$  the speed of light and  $\vec{s}$  is the spin vector. The constant  $\eta$  defines the coupling with the spin and is defined as:

$$\eta = \frac{4dmc}{q\hbar} \quad (11)$$

For a muon immersed in a electric and magnetic field the EDM introduces a torque which causes the spin precession plane to be tilted. The extra contribution to the precession in Eq 4:

$$\vec{\omega}_\eta = -\frac{q}{mc} \frac{\eta_\mu}{2} \left[ \vec{E} - \frac{\gamma}{1+\gamma} (\vec{\beta} \cdot \vec{E}) \vec{\beta} + c \vec{\beta} \times \vec{B} \right] \quad (12)$$

This leads to a total precession frequency of:

$$\vec{\omega}_{a\eta} = \vec{\omega}_a + \vec{\omega}_\eta = -\frac{q}{m} \left[ a_\mu \vec{B} + \frac{\eta_\mu}{2} (\vec{\beta} \times \vec{B}) \right] \quad (13)$$

Fig 5 shows a visual representation of the total precession frequency. Assuming a vertical magnetic field and longitudinal

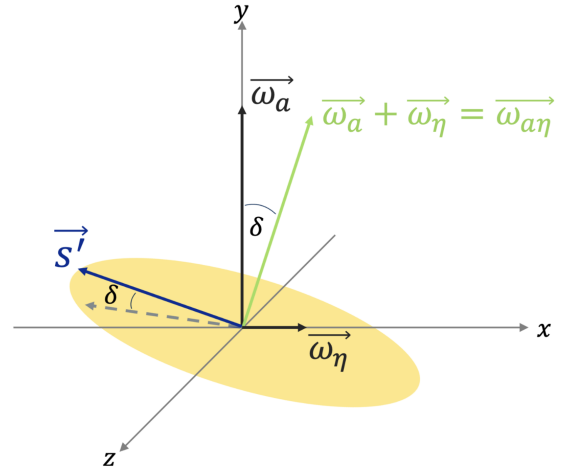


**FIGURE 5:** Visual explanation of the EDM tilt angle.

momentum the tilt angle in the spin precession plan is  $\delta = \tan^{-1} \frac{\omega_\eta}{\omega_a} \approx \frac{\beta \eta_\mu}{2a_\mu}$  so in the small angle approximation the EDM can be expressed as a function of the tilt angle:

$$d_\mu = \frac{q\hbar a_\mu}{2m_\mu c \beta} \delta \quad (14)$$

Any tilt in the precession plane causes an oscillation in the average vertical decay angle  $\langle \theta_y \rangle = \langle p_y / |p| \rangle$  and this is maximized when the spin and momentum are orthogonal, the contrary to the positron spectrum oscillation. This measurement is possible thanks to the straw trackers' information that can measure the momentum of each decay positron. Analysis of the Run-23 dataset is currently underway. The BNL experiment previously established a limit of  $|d_\mu| < 1.9 \times 10^{-19} \text{ e} \cdot \text{cm}$  [11], and the Muon  $g - 2$  experiment at Fermilab is projected to reach a final sensitivity of  $|d_\mu| < 3 \times 10^{-20} \text{ e} \cdot \text{cm}$ .

The EDM search is not the only BSM analysis conducted in the Muon  $g - 2$  experiment. Two additional analyses are sensitive to CPT and Lorentz Violation (CPTLV) and to scalar light dark matter. CPTLV arises from the Standard Model Extension (SME), which suggests that the vacuum is filled with vector

quantities oriented in four dimensions, leading to spontaneous symmetry breaking [20]. A muon precession in a magnetic field will encounter different orientations of these vectors as the Earth completes its rotation over a sidereal day. Measuring the oscillation amplitude of the spin precession rate at the sidereal frequency, or its harmonics, provides a probe to test the validity of SME theory. The sidereal oscillation amplitude in run-by-run data from the combined 1999/2000 BNL run was 2.2 ppm [21], from Fermilab measurements a 4.4 times improvement is expected. Similar to the case of CPTLV, a scalar or pseudo-scalar dark matter (DM) field would manifest as a modulation of  $\omega_a$ . In particular, a pseudo-scalar DM field would induce an oscillation perpendicular to the precession caused by the muon anomaly, analogous to the out-of-plane precession component generated by an EDM.

## ACKNOWLEDGEMENTS

This work was supported in part by the US DOE, Fermilab, the National Science Foundation (USA), the Science and Technology Facilities Council (UK), the Royal Society (UK), the European Union Horizon 2020 research and innovation programme under the Marie Skłodowska-Curie grant agreement No. 101006726, and the Leverhulme Trust, LIP-2021-014.

## References

- [1] D. P. Aguillard et al., “Measurement of the Positive Muon Anomalous Magnetic Moment to 127 ppb” PRL 135, 101802 (2025).
- [2] P. A. M. Dirac, “The quantum theory of electron. Part II”, Proc. R. Soc. A 118, 351 (1928).
- [3] J. S. Schwinger, “On quantum electrodynamics and the magnetic moment of the electron”, Phys. Rev. 73, 416 (1948).
- [4] R. Aliberti et al., “The anomalous magnetic moment of the muon in the Standard Model: an update”, arXiv:2505.21476 (2025).
- [5] T. Coffin, R. L. Garwin, S. Penman, L. M. Lederman, and A. M. Sachs, “Magnetic moment of the free muon”, Phys. Rev. 109, 973 (1958).
- [6] R. L. Garwin, D. P. Hutchinson, S. Penman, and G. Shapiro, “Accurate determination of the magnetic moment”, Phys. Rev. 118, 271 (1960).
- [7] J. M. Cassels, T. W. O’Keeffe, M. Rigby, A. M. Wetherell, and J. R. Wormald, “Experiments with a polarized muon beam”, Proc. Phys. Soc. London Sect. A 70, 543 (1957).
- [8] G. Charpak, F. J. M. Farley, R. L. Garwin, T. Muller, J. C. Sens, and A. Zichichi, “The anomalous magnetic moment of the muon: A world average value”, Nuovo Cimento 37, 1241 (1965).
- [9] J. Bailey, W. Bartl, G. Von Bochmann, R. Brown, F. Farley, H. Jöstlein, E. Picasso, and R. Williams, “Precision measurement of the anomalous magnetic moment of the muon”, Phys. Lett. 28B, 287 (1968).
- [10] J. Bailey et al. (CERN-Mainz-Daresbury Collaboration), “Final report on the CERN muon storage ring including the anomalous magnetic moment and the electric dipole moment of the muon, and a direct test of relativistic time dilation”, Nucl. Phys. B150, 1 (1979).
- [11] G. W. Bennett et al., “Final report of the E821 muon anomalous magnetic moment measurement at BNL”, Phys. Rev. D 73, 072003 (2006).
- [12] V. Bargmann, L. Michel, and V. Telegdi, “Precession of the Polarization of Particles Moving in a Homogeneous Electromagnetic Field”, Phys. Rev. Lett. 2, 435 (1959).
- [13] A.P. Schreckenberger et al., “The fast non-ferric kicker system for the Muon g-2 Experiment at Fermilab” Nucl. Instrum. Meth. A1011, 165597(2021).
- [14] P. J. Mohr, E. Tiesinga, D. B. Newell, and B. N. Taylor, “CODATA recommended values of the fundamental physical constants: 2022”, Rev. Mod. Phys. 97, 025002 (2025).
- [15] D. P. Aguillard et al., “Detailed report on the measurement of the positive muon anomalous magnetic moment to 0.20 ppm” PRD 110, 032009 (2024).
- [16] A. Anastasi et al “The laser-based gain monitoring system of the calorimeters in the Muon g-2 experiment at Fermilab” JINST 14 P11025 (2019).
- [17] On Kim et al., “Reduction of coherent betatron oscillations in a muon g-2 storage ring experiment using RF fields” New J. Phys. 22 063002 (2020).
- [18] T. Aoyama et al, “The anomalous magnetic moment of the muon in the Standard Model”, Phys. Rept. 887, 1 (2020).
- [19] F. V. Ignatov et al. (CMD-3 Collaboration), “Measurement of the pion form factor with CMD-3 detector and its implication to the hadronic contribution to Muon (g-2)”, Phys. Rev. Lett. 132, 231903 (2024).
- [20] Don Colladay and V. Alan Kostelecký “CPT violation and the standard model.” Phys. Rev. D, 55:6760–6774 (1997).
- [21] G. W. Bennett et al. “Search for Lorentz and CPT Violation Effects in Muon Spin Precession.” Phys. Rev. Lett., 100:091602 (2008).